JMRI
JMRI 2017; **00**:1–9
DOI:10.1002/jmri.25719

ORIGINAL RESEARCH

Valve mediated hemodynamics and their association with distal ascending aortic diameter in bicuspid aortic valve subjects

Vrishank Raghav, PhD*, Alex J Barker, PhD†, Daniel Mangiameli, BS*, Lucia Mirabella, PhD*, Michael Markl, PhD†, Ajit P. Yoganathan, PhD*

*Georgia Institute of Technology, Atlanta, GA, USA; †Northwestern University, Evanston, IL, USA.

ABSTRACT

Purpose: Valve mediated hemodynamics have been postulated to contribute to pathology of the Ascending Aorta (AAo). The objective of this study is to assess the association of aortic valve morphology and hemodynamics with downstream AAo size in subjects with bicuspid aortic valve (BAV) disease.
Materials and Methods: Four-dimensional flow MRI at 1.5 or 3T was used to evaluate the hemodynamics in the proximal AAo of 52 subjects: size-matched controls with tricuspid aortic valves (n = 24, mid ascending aorta (MAA) diameter = 38.0±4.9 mm) and BAV patients with aortic dilatation (n = 14 RL-BAV, MAA diameter = 38.1±5.3 mm; n = 14 RN-BAV, 36.5±6.6 mm). A validated semi-automated technique was used to evaluate hemodynamic metrics (flow angle, flow displacement, and jet quadrant) and valve morphology (orifice circularity) for all subjects. Regression analysis of these metrics to AAo diameter was performed.
Results: RN-BAV subjects displayed a stronger correlation between hemodynamic metrics in the proximal AAo with diameter in the distal AAo compared to size-matched TAV controls and RL-BAV subjects. The distal AAo diameter was found to be strongly correlated to the upstream flow displacement ($R^2{}_{adjusted} = 0.75$) and flow angle ($R^2{}_{adjusted} = 0.66$) measured at the sino-tubular junction (STJ). Orifice circularity was also strongly correlated ($R^2{}_{adjusted} = 0.53$) to the distal AAo diameter in RN-BAV subjects. For TAV controls and RL-BAV subjects, correlations were weaker ($R^2{}_{adjusted} < 0.2$).
Conclusions: Hemodynamics in the STJ were strongly correlated to the distal AAo diameter for the RN-BAV subjects. Hemodynamic metrics were more strongly correlated to the downstream aortic size when compared to valve morphology metrics.

KEYWORDS

bicuspid aortic valve, valve fusion pattern, flow displacement, aortic diseases, hemodynamics, 4D flow MRI

Correspondence

Ajit P. Yoganathan, PhD, ajit.yoganathan@bme.gatech.edu

Received 12/30/2016. Accepted 3/16/2017

INTRODUCTION

Bicuspid aortic valve (BAV) is the most common congenital heart defect, affecting 1-2% of the US population [1]. The morphology of BAV is often classified based on valve leaflet fusion patterns, such as: a) right and left coronary leaflet fusion (RL 80% incidence), b) right and non-coronary leaflet fusion (RN 17% incidence), and c) left and non-coronary leaflet fusion (LN 2% incidence) [2, 3]. Complications of BAV include valvular calcification, stenosis, regurgitation, aortic root dilatation, and/or aortic aneurysm [4, 5].

The pathophysiologic mechanisms underlying the risk of aortopathy in BAV patients have yet to be clearly identified [6, 7, 8, 9, 10]. One in a hundred BAV patients per year are thought to have an ascending aortic aneurysm, with the current guidelines driving the prophylactic replacement of the ascending aorta in approximately 25% of patients [11, 12]. These guidelines have largely been developed based on the assumption of a genetic origin for aortopathy [13]. Nonetheless, uncertainty surrounding a solely genetic origin has spawned alternative hypotheses, such as the hemodynamic hypothesis, which postulates that altered BAV morphology creates focal areas of disease within the aortic wall related to abnormal transvalvular blood flow [14]. Corroborating this concept, recent studies have demonstrated a correlation between hemodynamic metrics dependent on leaflet fusion patterns such as wall

shear stress, flow displacement, and flow angle and the phenotype of aortopathy in BAV subjects [15, 16, 17, 18, 19, 20]. However, most of these studies have only evaluated hemodynamic metrics in the vicinity of the hypothesized aortopathy, in order to investigate a possible link between hemodynamics and regional BAV aortopathy. The specific role of the valve morphology and valve-related hemodynamic metrics on distal Ascending Aorta (AAo) aortopathy has not been investigated in previous studies such as Barker et al. [14], Mahadevia et al. [18], Hope et al. [16, 19]. For example, the influence of valve fusion phenotype, valve opening area, or opening eccentricity on hemodynamic metrics through the AAo needs additional investigation to understand the relationship to distal aortic remodeling (e.g. aortic size). Such a comprehensive understanding could help optimize the implementation of standard of care imaging protocols (i.e. short 2D acquisitions over the longer 4D flow MRI acquisitions). In order to achieve these goals, the aim here was to use a location commonly imaged as a part of standard of care to understand the impact of the upstream valve morphology and hemodynamics on the distal AAo geometry and hemodynamics using 4D flow MRI data. Furthermore, this study uses a novel semi-automated MRI data processing technique [21] that was not previously used in the studies by Barker et al. [14] and Mahadevia et al. [18].

MATERIALS AND METHODS

Study Cohort

Fifty-two patients were retrospectively chosen from a database of 151 patients that underwent cardiac MRI to assess aortic dimensions or aortic valve morphology and function. They were categorized into three groups of subjects consisting of 24 subjects with normal tricuspid aortic valves and aortic dilatation (age = 58.2±13.3, 4 females) to serve as aorta size-matched controls for BAV subjects, 14 RL-BAV subjects (age = 47.2±11.9, 3 females), and 14 RN-BAV subjects (age = 44.7±8.3, 4 females). Exclusionary criteria for all the groups included aortic stenosis or insufficiency greater than moderate. Aortic dilatation was defined as a sinus of Valsalva diameter $>$ 40 mm or MAA diameter $>$ 40 mm. The severity of aortic stenosis or insufficiency was determined by a radiologist with 10 years of experience using standard-of-care imaging described in the next sub-section. Patients were included in accordance with an institutional review board protocol which permitted retrospective chart review with waiver of consent.

MRI Data Acquisition

All subjects underwent cardiac MRI at 1.5T or 3T (Magnetom Espree, Avanto, Skyra or Trio Siemens Medical Systems, Germany). Cardiac MRI included ECG-gated, two-dimensional breathheld balanced steady-state free precessing (bSSFP) cine imaging to assess BAV morphology as described previously [22]. In addition, 3D phase-contrast MRI, with three-directional velocity encoding (4D flow MRI) was acquired in a sagittal oblique volume covering the thoracic aorta. Prospective ECG gating was used with a respiratory navigator placed on the lung-liver interface. Pulse sequence parameters were as follows: flip angle of 15°, spatial resolution of 1.73.7 mm by 1.82.6 mm by 2.23.7 mm, temporal resolution of 36.843.2 ms, total acquisition time, 8-15 minutes depending on heart rate and navigator efficiency, and velocity encoding range of 13 m/s.

Post-processing and Data Analysis

The cine and 4D flow MRI data were processed using a recently validated semi-automated technique designed to extract aortic valve and aorta morphometry and hemodynamics [21]. Post-processing of the MRI data was composed of the following steps: 2D bSSFP cine image analysis, preprocessing of the 4D flow data, and spatial registration of the 2D to the 3D data, and finally, the extraction of 3D geometric and hemodynamic metrics. Similar to our previous work [21], the metrics derived from the MRI data included: a) hemodynamics i.e mean velocity, flow angle, flow displacement, and jet quadrant and b) geometric valve morphology (area, circularity, eccentricity of the valve orifice) and aorta diameter. These values were evaluated at 11 equally spaced cross-sections (S_{0-10}) downstream from the valve annulus as illustrated in Figure 1A. The sino-tubular junction (S_2 in Figure 1A) was used as a location to evaluate the hemodynamic metrics since the flow was better defined and the effect of aortic valve leaflet interference with the acquisition plane was minimized at this location. Furthermore, the sino-tubular junction was chosen to replicate potential sites of imaging for standard of care MRI. The robustness of this technique was evaluated by quantifying the intra observer differences [21].

Statistical Analysis

For each group (aorta size-matched TAV controls, RL-BAV, and RN-BAV), a Shapiro-Wilk test was used to determine if the parameters were normally distributed. One-way ANOVA was used to compare hemodynamic and geometric parameters between the three groups ($p < 0.05$ was considered significant). Univariate and multivariate regression models were tested for each group to correlate geometric and hemodynamic metrics with distal AAo diameter. The quality of the data has been adjusted for the number of subjects in the analysis and hence the goodness of fit in the regression analysis is reported as ${R^2}_{adjusted}$, a conservative estimate when compared to R^2. ${R^2}_{adjusted} > 0.5$ was considered a strong correlation, $0.2 < {R^2}_{adjusted} < 0.5$ was considered a moderate correlation, and ${R^2}_{adjusted} < 0.2$ was considered a weak correlation. Statistical analysis was performed using MATLAB (Release 2012b, The MathWorks Inc., Natick, Massachusetts, United States).

JMRI 2017; **00**:1–9
DOI: 10.1002/jmri
Prepared using LaTeX

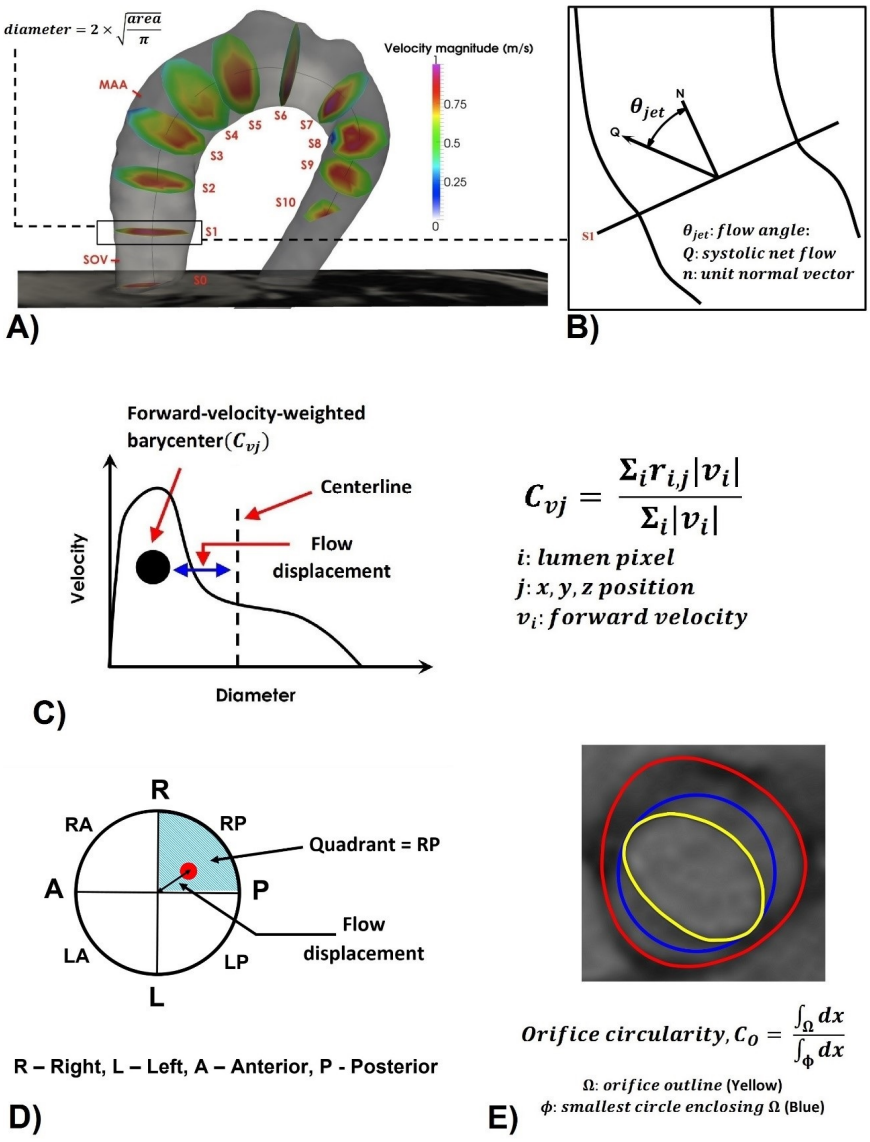

Figure 1. A) Illustration of different cross sections at which the analysis was performed, B) definition of systolic flow angle, C) definition of forward-velocity-weighted barycenter and flow displacement, D) definition of jet quadrant shown in the top view of the aortic cross-section and E) definition of orifice circularity (Co)

RESULTS

Study Cohort

The demographics of the study cohort are summarized in Table I. Size-matched TAV subjects were significantly ($p < 0.02$) older than patients with BAV. The MAA diameter (Section S3 in Figure 1A) among all the groups were not significantly different ($p > 0.5$). Aortic stenosis severity was mild (n =0, 2, 2) and moderate (n =2, 1, 2) for TAV, RL-BAV, and RN-BAV subjects respectively. Aortic insufficiency was present in (n = 7) of TAV, (n = 7) of RL-BAV, and (n = 9) of RN-BAV subjects. Eccentricity of the orifice was significantly larger in RN-BAV than TAV ($2.\pm1.1$ vs. 3.9 ± 1.6, $p < 0.02$). A summary of the variation of mean geometric and hemodynamic parameters at all cross sections downstream of the aortic valve is illustrated in Figure 2. Normalized flow displacement at the sino-tubular junction (STJ) was significantly larger in both RL and RN BAV subjects than size-matched TAV (0.17 ± 0.08 and 0.18 ± 0.10 vs. $0.11\pm.08$, $p < 0.02$). Flow angle measured at the STJ was not significantly different among the three groups ($p > 0.15$). The jet quadrant distribution evaluated at the STJ for the RL-BAV patients was predominantly in the RA quadrant and was distributed across all quadrants in RN-BAV subjects. The jet quadrant for size-matched controls was primarily central, as per observations from

Table I. Summary of patient demographics, aortic dimensions, valve geometry and hemodynamic characteristics. All continuous data are presented as mean standard deviation. *Independent-sample t test indicates significant differences compared with size-matched controls ($p < 0.02$). MAA – mid ascending aorta, SOV – sinus of valsalva, STJ – sino-tubular junction, C – central, RA – right anterior, RP – right posterior, LA – left anterior, LP – left posterior.

		TAV	RL-BAV	RN-BAV
n(female)		24(4)	14(3)	14(4)
Age		58.2±13.3	47.2±11.9*	44.7±8.3*
MAA diameter, mm		38.0±4.9	38.1±5.3	36.5±6.6
SOV diameter, mm		42.3±4.6	40.5±2.7	43.9±4.9
Stenosis severity	Mild	0	2	2
	Moderate	2	1	2
	Severe	0	0	0
Aortic insufficiency	Mild	4	5	6
	Moderate	3	2	3
	Severe	0	0	0
Orifice eccentricity,		2.0±1.1	2.0±1.0	3.9±1.6*
Orifice circularity,		0.59±0.10	0.62±0.13	0.57±0.14
Normalized flow displacement at STJ		0.11±0.08	0.19±0.07*	0.18±0.11*
Flow angle at STJ°		18.2±10.5	23.5±10.3	22.1±17.9
Jet quadrant at STJ		C-15, RA-1, RP-7, LA-1, LP-0,	C-2, RA-7, RP-4, LA-1	C-2, RA-5, RP-4, LA-2, LP-1

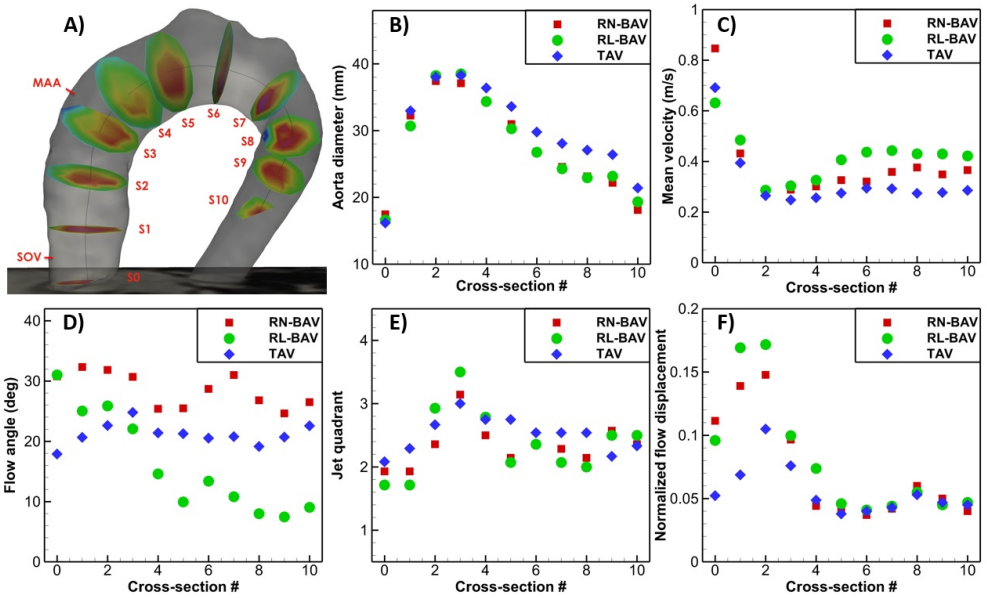

Figure 2. Summary of the variation of mean geometric and hemodynamic parameters at all cross sections downstream of the aortic valve for all the groups of subjects: A) Illustration of the cross sections, B) aortic diameter, C) mean velocity at centerline, D) flow angle, E) jet quadrant, F) normalized flow displacement.

previous studies where a normalized flow displacement $<$ 0.1 was considered central [23].

Correlation Between Hemodynamics and Ascending Aorta Diameter

Two hemodynamic metrics (flow displacement and flow angle, defined in Figure 1) evaluated at the STJ (S_2, Figure 1A) correlated well ($R^2{}_{adjusted} > 0.5$) to the distal AAo (S_4-S_6) diameter. Figure 3 illustrates the best regression results between normalized flow displacement at S_2 and aorta diameter at S_5 for the three groups. It was observed that all the groups had a positive association between normalized flow displacement at the STJ and distal AAo (S_5) diameter. RN-BAV subjects had the highest correlation with a significant positive association ($R^2{}_{adjusted} = 0.75$, slope = 54.8, $p < 0.01$), RL-BAV subjects had the weakest correlation ($R^2{}_{adjusted} = 0.01$),

JMRI 2017; **00**:1–9
DOI: 10.1002/jmri
Prepared using LaTeX

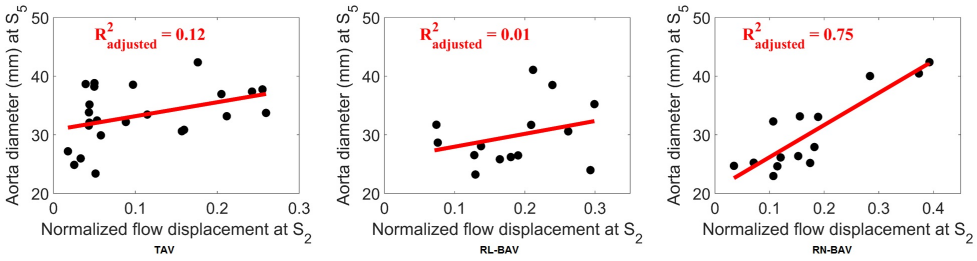

Figure 3. Association between normalized flow displacement at S2 and aorta diameter at S5.

Table II. Summary of linear regression coefficients for the correlation between normalized flow displacement at S_2 and aortic diameter at downstream cross-sections. $^{\dagger}p < 0.01$, $^{\star}p < 0.055$

Cross-section	TAV		RL-BAV		RN-BAV	
	$R^2{}_{adjusted}$	Slope	$R^2{}_{adjusted}$	Slope	$R^2{}_{adjusted}$	Slope
S_2	0.00	10.2	0.00	18.7	0.18	33.5
S_3	0.18	$28.0^{\star}$	0.15	34.1	0.42	$42.8^{\dagger}$
S_4	0.18	$24.4^{\star}$	0.07	24.8	0.62	$50.3^{\dagger}$
S_5	0.12	$23.8^{\star}$	0.01	21.9	0.75	$54.8^{\dagger}$
S_6	0.03	14.1	0.00	7.6	0.70	$37.7^{\dagger}$

and aorta size-matched TAV subjects had a moderately better correlation ($R^2{}_{adjusted} = 0.12$, slope = 23.8, $p < 0.055$).

Two hemodynamic metrics (flow displacement and flow angle, defined in Figure 1) evaluated at the STJ (S_2, Figure 1A) correlated well ($R^2{}_{adjusted} > 0.5$) to the distal AAo (S_4-S_6) diameter. Figure 3 illustrates the best regression results between normalized flow displacement at S_2 and aorta diameter at S_5 for the three groups. It was observed that all the groups had a positive association between normalized flow displacement at the STJ and distal AAo (S_5) diameter. RN-BAV subjects had the highest correlation with a significant positive association ($R^2{}_{adjusted} = 0.75$, slope =54.8, $p < 0.01$), RL-BAV subjects had the weakest correlation ($R^2{}_{adjusted} = 0.01$), and aorta size-matched TAV subjects had a moderately better correlation ($R^2{}_{adjusted} = 0.12$, slope = 23.8, $p < 0.055$).

Table II summarizes the linear regression results for the correlation between normalized flow displacement at the STJ and downstream aortic diameter at S_{3-6}. RN-BAV subjects exhibited a positive association between normalized flow displacement and aortic diameter; an increase in normalized flow displacement at the STJ was observed to cause a significant increase ($p < 0.01$) in downstream aortic diameter at cross-sections S_{3-6}. Although the goodness of fit was relatively lower for TAV subjects when compared to RN-BAV subjects, the data exhibited a positive trend ($p < 0.055$). Normalized flow displacement was observed to have a negligible impact on the downstream aorta diameter for RL-BAV subjects. The most noteworthy observation here is that the flow displacement at the STJ is strongly associated with the AAo diameter at S_5 for RN-BAV subjects.

Furthermore, the flow angle for RN-BAV subjects at the STJ had the highest correlation and a significant positive association ($R^2{}_{adjusted} = 0.66$, slope =0.32, $p < 0.01$) with the diameter of the AAo at section S_4 (Figure 4). RL-BAV subjects exhibited a weak correlation ($R^2{}_{adjusted} = 0.16$, slope =0.23, $p < 0.1$), while TAV subjects had the weakest correlation ($R^2{}_{adjusted} = 0.04$). Table III summarizes the regression data between flow angle at the STJ and aortic diameter at downstream cross-sections. Flow angle strongly correlated to most of the distal portions of the AAo (S_{3-5}) for RN-BAV subjects, while the strongest correlation for RL-BAV subjects was observed at the immediately following cross-section (S_3). However, it should be noted that the significance of the positive association between flow angle and AAo diameter was markedly different between the two groups, $p < 0.01$ vs $p < 0.1$ for RN-BAV and RL-BAV subjects respectively.

Correlation Between Valve Morphology and Ascending Aorta Diameter

It was observed that valve orifice circularity best correlated with downstream AAo diameter. Figure 5 illustrates the best regression results between orifice circularity and AAo diameter at the STJ for the three groups. It was observed that RN-BAV subjects had the highest correlation with a significant negative association ($R^2{}_{adjusted} = 0.53$, slope =-36.9, $p < 0.01$), RL-BAV subjects had the weakest correlation ($R^2{}_{adjusted} = 0.00$), and aorta size-matched TAV subjects had a moderate correlation with negative association ($R^2{}_{adjusted} = 0.26$, slope =-26.5, $p < 0.06$).

Table IV summarizes the linear regression results for the correlation between orifice circularity and downstream aortic diameter at S_{2-6}. RN-BAV subjects exhibited a negative association between orifice circularity and

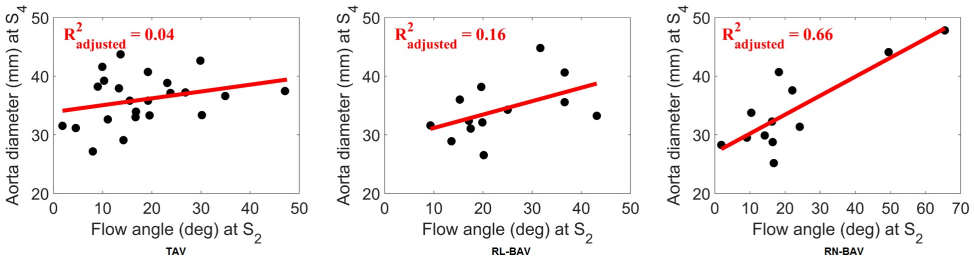

Figure 4. Association between flow angle at S2 and aorta diameter at S4.

Table III. Summary of linear regression coefficients for the correlation between flow angle at S_2 and aortic diameter at downstream cross-sections. $^{\dagger}p < 0.01$

Cross-section	TAV		RL-BAV		RN-BAV	
	$R^2{}_{adjusted}$	Slope	$R^2{}_{adjusted}$	Slope	$R^2{}_{adjusted}$	Slope
S_2	0.18	0.21	0.00	0.00	0.39	0.27
S_3	0.09	0.16	0.21	0.26	0.53	$0.30^{\dagger}$
S_4	0.04	0.11	0.16	0.23	0.66	$0.32^{\dagger}$
S_5	0.00	0.06	0.00	0.15	0.49	$0.29^{\dagger}$
S_6	0.00	0.03	0.00	0.05	0.34	0.18

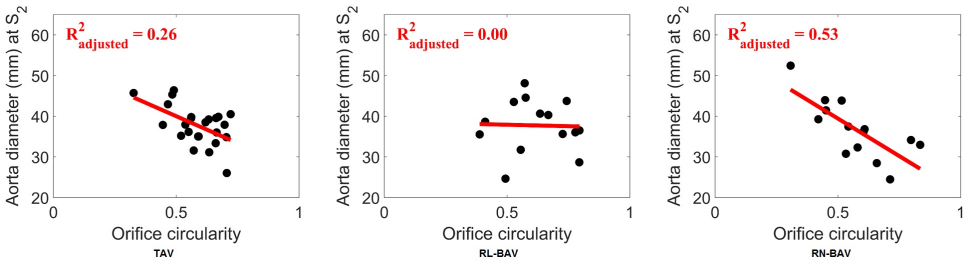

Figure 5. Association between orifice circularity and aorta diameter at S_2.

Table IV. Summary of linear regression coefficients for the correlation between orifice circularity and aortic diameter at downstream cross-sections. $^{\dagger}p < 0.01$, $^{\star}p < 0.055$

Cross-section	TAV		RL-BAV		RN-BAV	
	$R^2{}_{adjusted}$	Slope	$R^2{}_{adjusted}$	Slope	$R^2{}_{adjusted}$	Slope
S_2	0.26	$-26.5^{\star}$	0.00	-1.43	0.53	$-36.9^{\star}$
S_3	0.16	$-22.1^{\dagger}$	0.00	-10.4	0.28	$-26.4^{\dagger}$
S_4	0.07	-14.4	0.07	-13.1	0.20	$-23.3^{\dagger}$
S_5	0.00	-2.0	0.01	-11.6	0.05	-15.8
S_6	0.00	3.1	0.06	-4.88	0.00	-0.6

AAo diameter; a more circular annulus was observed to be associated with a significant decrease ($p < 0.01$) in downstream aortic diameter at cross-sections S_{2-4}. Although the goodness of fit was relatively lower for TAV subjects when compared to RN-BAV subjects ($R^2{}_{adjusted} = 0.53$ vs 0.26), the data exhibited a significant negative association ($p < 0.06$). Furthermore, orifice circularity was observed to have no impact on the AAo diameter for RL-BAV subjects.

Multivariate Regression Analysis

The two strongly correlated hemodynamic variables flow angle and flow displacement along with a valve morphology variable (i.e. orifice circularity) were used for this multiple regression analysis (Table V summarizes the results of this analysis). The strongest correlations in the multivariate analysis were observed in the RN-BAV subjects when compared with RL-BAV subjects and size-matched TAV controls ($R^2{}_{adjusted} = 0.79$ vs 0.11 vs 0.18). Normalized flow displacement and flow angle were observed to have the most significant impact for RN-BAV subjects.

JMRI 2017; **00**:1–9
DOI: 10.1002/jmri
Prepared using LaTeX

Table V. Summary of linear multiple regression analysis of the strongly AAo hemodynamic and valve geometric variables with distal AAo diameter (S_4).$^\star p < 0.05$

		Reg. coeff. (β)		
Subject cohort	Mult. Reg. $R^2{}_{adjusted}$	Orifice Circ.	Flow Disp. at S_2	Flow angle at S_2
TAV	0.18	-11.45	22.61*	0.03
RL-BAV	0.11	-13.72	7.91	0.11
RN-BAV	0.79	-7.07	28.43*	0.18*

DISCUSSION

This study utilized a validated semi-automated 4D flow MRI processing technique [21] to analyze a cohort of patients to understand the relationship of BAV valve phenotypes and their association to downstream hemodynamics and AAo geometry. The development of such relationships could help further improve prognostic hemodynamic metrics for BAV subjects using less complex standard of care 2D imaging protocols [24] – for example a dynamic cine or phase-contrast MRI at the level of the aortic valve and/or STJ which could provide prognostic morphologic or hemodynamic information. For these reasons, we focused on measuring upstream parameters that are capable of being acquired using standard of care 2D PC-MRI imaging planes at the level of the STJ. The relationship of these measurements to downstream aortic diameter was assessed via a regression analysis. Additionally, the STJ was used as a location to evaluate the hemodynamic metrics since the flow was better defined and the effect of aortic valve leaflet interference with the flow was minimum at this location. The user variability of the manual segmentation process was assessed in a blind test by two other members of the research group [21].

Similar to previous findings [17, 18, 19], the presence of BAV and the type of cusp fusion pattern were accompanied by changes in systolic hemodynamic metrics as quantified by flow displacement and flow angle in the STJ. The values of normalized flow displacement at the STJ are in the range of values reported previously for BAV subjects [23, 24]. Systolic hemodynamic metrics in the STJ were strongly correlated with the distal AAo diameter in the RN-BAV patients, while RL-BAV patients and size-matched TAV controls exhibited weak-moderate associations to aortic size. These observations corroborate prior work [17, 18], where the systolic jet in RN-BAV subjects has been observed to reflect off of the inner curvature of the proximal AAo before impinging on the distal AAo which could be the primary cause for the observed correlation.

The findings are intriguing in that upstream hemodynamic alterations in the RN-BAV group appeared to be most correlated to distal AAo diameter, while the RL-BAV group did not display an association of upstream hemodynamics with downstream aortic size. This is of particular interest because the RLBAV group is thought to exhibit dilation in the root and sinus regions [17]. Thus, the poor correlation of the RL-BAV group to downstream diameter observed in this work may be either an artifact of the automated PC-MRA approach to measure diameter in the sinus region, or simply be associated with inherent underlying genetic differences of the RL valve phenotype and their response to hemodynamic stressors. Garcia et al. previously investigated the use of a similar automated PC-MRA approach to estimate aortic diameter and found excellent agreement throughout the aorta as compared to the standard manual CE-MRA approach, except at the sinus of Valsalva region (SOV) [25]. This may have confounded the correlations between upstream hemodynamics and SOV diameter extracted using the automated PC-MRA approach used here, especially among the RL-BAV group. Thus, we also investigated the correlation of upstream hemodynamics with SOV diameter measurements obtained manually with CE-MRA for both RL and RN-BAV patients. We still found relatively poor agreement between the upstream hemodynamic measurements and the downstream aortic diameter for RL-BAV patients when compared to RN-BAV patients. This comparative analysis demonstrates that the poor correlation of upstream hemodynamics to downstream diameter observed for the RL-BAV group may not be an artifact of the PC-MRA approach. Hence, the poor correlation might be associated with underlying genetic differences of the RL-BAV group and their unresponsiveness to altered hemodynamics. Moreover, it has been postulated that isolated dilation of the aortic root and sinus regions for RL-BAV patients may be related to intrinsic genetic abnormalities of tissue rather than altered hemodynamics, such as seen in Marfan patients [6, 26].

A similar pattern for the TAV, RL-BAV, and RN-BAV cohorts was found when examining valve morphology. For example, orifice circularity was observed to be associated strongly with the downstream AAo diameter for RN-BAV subjects. However, other descriptors of valve morphology (area, eccentricity) were not associated with downstream AAo diameter. Similar to the hemodynamic metrics, the circularity of the orifice did not vary significantly between subject cohorts, however, RN-BAV subjects did exhibit a strong correlation between valve orifice circularity and downstream AAo diameter. Unlike hemodynamic metrics, valve orifice circularity was strongly correlated only to the diameter of the proximal portions of the AAo (close to STJ) and not to the distal portions of the AAo. Again, the relationships indicate that only the RN-BAV cohort showed a relationship between upstream hemodynamics and valve geometry to downstream aortic size. Acknowledging that the study numbers are limited in size, future studies investigating the relationship of hemodynamics to aortic

remodeling should be cognizant of these interesting findings.

Multivariate regression analysis did not reveal significant correlations in the RL-BAV or size-matched TAV control subjects nor did it significantly improve the regressions quality. Among the RN-BAV subjects, systolic hemodynamics (flow displacement and flow angle) in the proximal AAo played a more critical role, than the valve geometric metrics (orifice circularity). This finding suggests the systolic hemodynamic metrics (as opposed to valve geometry) in the proximal AAo are sufficient as upstream parameters to further investigate distal AAo remodeling. Flow displacement or flow angle alone might not be sufficient to explain all the observations in this work; knowledge of the orientation of the displacement or flow angle requires an additional descriptor. Thus, jet quadrant was used to measure the direction of the jet or flow eccentricity. In brief, Jet quadrant is an indication of the direction (RA, LA, RP, LP) of the flow displacement. Since the direct assessment of wall shear stress (WSS) was not investigated in this study due to the focus on parameters that can be derived using standard of care 2D PC MRI, WSS data from prior work has been compared to the jet quadrant data from this work. It was observed that the jet quadrant distribution for flow displacement in RL-BAV patients was predominantly in the RA quadrant and in the RP quadrant for RN-BAV patients, agreeing with previously reported WSS distributions at the level of the STJ [18]. While this information is useful, it suggests that flow displacement and jet quadrant can be used to only derive an understanding of WSS at the same location, but does not provide any information about the downstream location. Significant flow displacement implies elevated WSS at the same location, not where the vessel diameter is larger at the downstream location.

Implications on BAV diagnosis and treatment include insights provided by this work into the resulting downstream effects of valve abnormalities caused by BAV. These results could be used to optimize standard of care imaging protocols (for example 2D PC-MRI at the level of the STJ), as demonstrated by recent reports [23] to measure changes in distal AAo diameter. With further validation and based on recent results reporting prognostic significance [24], the findings in this work suggest that the presence of flow abnormalities in the proximal AAo might be a time-efficient approach to risk-stratify certain subsets of BAV patients. Using future longitudinal studies, this approach could help fine-tune risk assessment such that preemptive patient specific surveillance intervals and therapeutic strategies can be determined within a feasible imaging window and realistic analysis timeline.

There are several potential limitations in this study. Longitudinal studies are critical to improve the current understanding of the relationship between BAV phenotype/morphology to aortopathy risk stratification. In order to connect the diagnostic suggestions in this work, the evaluation of better indicators of remodeling (for example WSS) should to be considered in the distal AAo and correlated to flow displacement and/or flow angle in the proximal AAo. However, this work was an initial investigation of readily obtainable parameters and the measurement of WSS was not within the scope of this work. Furthermore, limitations of the study due to small subject cohort and inherent biases of a retrospective study should be noted.

In conclusion, the current study has shown that hemodynamics at the STJ are significantly correlated to the distal AAo diameter in RN-BAV subjects. Furthermore, the measurement of upstream hemodynamic metrics demonstrated more statistical significance than geometric metrics of the valve orifice when considering correlations to downstream aortic size. The findings in this work could be used to design efficient imaging protocols for better prognosis of BAV-related aortopathy.

ACKNOWLEDGEMENT

The authors would like to thank the members of the cardiovascular fluid mechanics laboratory. This study was supported by National Institutes of Health (NIH) National Heart, Lung, and Blood Institute (NHLBI) grant R01HL115828 and K25HL119608 and American Heart Association Postdoctoral Fellowship 16POST27520030.

REFERENCES

1. Fedak PW, Verma S, David TE, Leask RL, Weisel RD, Butany J. Clinical and pathophysiological implications of a bicuspid aortic valve. *Circulation* 2002; **106**(8):900–904.
2. Sievers HH, Schmidtke C. A classification system for the bicuspid aortic valve from 304 surgical specimens. *The Journal of Thoracic and Cardiovascular Surgery* 2007; **133**(5):1226–1233.
3. Schaefer BM, Lewin MB, Stout KK, Gill E, Prueitt A, Byers PH, Otto CM. The bicuspid aortic valve: an integrated phenotypic classification of leaflet morphology and aortic root shape. *Heart* 2008; **94**(12):1634–1638.
4. Mordi I, Tzemos N. Bicuspid aortic valve disease: a comprehensive review. *Cardiology research and practice* 2012; **2012**.
5. Ward C. Clinical significance of the bicuspid aortic valve. *Heart* 2000; **83**(1):81–85.
6. Girdauskas E, Borger MA, Secknus MA, Girdauskas G, Kuntze T. Is aortopathy in bicuspid aortic valve disease a congenital defect or a result of abnormal hemodynamics? a critical reappraisal of a one-sided argument. *European Journal of Cardio-Thoracic Surgery* 2011; **39**(6):809–814.
7. Michelena HI. The bicuspid aortic valve aortopathy mystery continues: Are we that mediocre? *Trends in cardiovascular medicine* 2015; **25**(5):452.
8. Sievers HH, Sievers HL. Aortopathy in bicuspid aortic valve diseasegenes or hemodynamics? or scylla and charybdis? 2011.

DOI: 10.1002/jmri
Prepared using LaTeX

9. Tadros TM, Klein MD, Shapira OM. Ascending aortic dilatation associated with bicuspid aortic valve. *Circulation* 2009; **119**(6):880–890.
10. Davies RR, Kaple RK, Mandapati D, Gallo A, Botta DM, Elefteriades JA, Coady MA. Natural history of ascending aortic aneurysms in the setting of an unreplaced bicuspid aortic valve. *The Annals of Thoracic Surgery* 2007; **83**(4):1338–1344.
11. Michelena HI, Khanna AD, Mahoney D, Margaryan E, Topilsky Y, Suri RM, Eidem B, Edwards WD, Sundt TM, Enriquez-Sarano M. Incidence of aortic complications in patients with bicuspid aortic valves. *Jama* 2011; **306**(10):1104–1112.
12. Opotowsky AR, Perlstein T, Landzberg MJ, Colan SD, OGara PT, Body SC, Ryan LF, Aranki S, Singh MN. A shifting approach to management of the thoracic aorta in bicuspid aortic valve. *The Journal of thoracic and cardiovascular surgery* 2013; **146**(2):339–346.
13. Hardikar AA, Marwick TH. The natural history of guidelines: the case of aortopathy related to bicuspid aortic valves. *International journal of cardiology* 2015; **199**:150–153.
14. Barker AJ, Markl M, Bürk J, Lorenz R, Bock J, Bauer S, Schulz-Menger J, von Knobelsdorff-Brenkenhoff F. Bicuspid aortic valve is associated with altered wall shear stress in the ascending aortaclinical perspective. *Circulation: Cardiovascular Imaging* 2012; **5**(4):457–466.
15. Bissell MM, Hess AT, Biasiolli L, Glaze SJ, Loudon M, Pitcher A, Davis A, Prendergast B, Markl M, Barker AJ, *et al.*. Aortic dilation in bicuspid aortic valve disease: flow pattern is a major contributor and differs with valve fusion type. *Circulation: Cardiovascular Imaging* 2013; :CIRCIMAGING–113.
16. Hope MD, Hope TA, Meadows AK, Ordovas KG, Urbania TH, Alley MT, Higgins CB. Bicuspid aortic valve: four-dimensional mr evaluation of ascending aortic systolic flow patterns 1. *Radiology* 2010; **255**(1):53–61.
17. Kang JW, Song HG, Yang DH, Baek S, Kim DH, Song JM, Kang DH, Lim TH, Song JK. Association between bicuspid aortic valve phenotype and patterns of valvular dysfunction and bicuspid aortopathy: comprehensive evaluation using mdct and echocardiography. *JACC: Cardiovascular Imaging* 2013; **6**(2):150–161.
18. Mahadevia R, Barker AJ, Schnell S, Entezari P, Kansal P, Fedak PW, Malaisrie SC, McCarthy P, Collins J, Carr J, *et al.*. Bicuspid aortic cusp fusion morphology alters aortic three-dimensional outflow patterns, wall shear stress, and expression of aortopathy. *Circulation* 2014; **129**(6):673–682.
19. Hope MD, Hope TA, Crook SE, Ordovas KG, Urbania TH, Alley MT, Higgins CB. 4d flow cmr in assessment of valve-related ascending aortic disease. *JACC: Cardiovascular Imaging* 2011; **4**(7):781–787.
20. Girdauskas E, Rouman M, Disha K, Fey B, Dubslaff G, Theis B, Petersen I, Gutberlet M, Borger MA, Kuntze T. Functional aortic root parameters and expression of aortopathy in bicuspid versus tricuspid aortic valve stenosis. *Journal of the American College of Cardiology* 2016; **67**(15):1786–1796.
21. Mirabella L, Barker AJ, Saikrishnan N, Coco ER, Mangiameli DJ, Markl M, Yoganathan AP. Mri-based protocol to characterize the relationship between bicuspid aortic valve morphology and hemodynamics. *Annals of biomedical engineering* 2015; **43**(8):1815–1827.
22. Malaisrie SC, Carr J, Mikati I, Rigolin V, Yip BK, Lapin B, McCarthy PM. Cardiac magnetic resonance imaging is more diagnostic than 2-dimensional echocardiography in determining the presence of bicuspid aortic valve. *The Journal of thoracic and cardiovascular surgery* 2012; **144**(2):370–376.
23. Burris NS, Hope MD. Bicuspid valve-related aortic disease: flow assessment with conventional phase-contrast mri. *Academic radiology* 2015; **22**(6):690–696.
24. Burris NS, Sigovan M, Knauer HA, Tseng EE, Saloner D, Hope MD. Systolic flow displacement correlates with future ascending aortic growth in patients with bicuspid aortic valves undergoing magnetic resonance surveillance. *Investigative radiology* 2014; **49**(10):635–639.
25. Garcia J, Barker AJ, Murphy I, Jarvis K, Schnell S, Collins JD, Carr JC, Malaisrie SC, Markl M. Four-dimensional flow magnetic resonance imaging-based characterization of aortic morphometry and haemodynamics: impact of age, aortic diameter, and valve morphology. *Eur Heart J Cardiovasc Imaging* 2015; :jev228.
26. Della Corte A, De Santo LS, Montagnani S, Quarto C, Romano G, Amarelli C, Scardone M, De Feo M, Cotrufo M, Caianiello G. Spatial patterns of matrix protein expression in dilated ascending aorta with aortic regurgitation: congenital bicuspid valve versus marfans syndrome. *J Heart Valve Dis* 2006; **15**(1):20–7.